Chalcogenide Letters Vol. 12, No. 6, June 2015, p. 287 - 300

EFFECT OF Nb_2O_5 NETWORK STABILIZER ON ELASTIC AND OPTICAL PROPERTIES OF $x$$Nb_2O_5$-(20-$x$)BaO-80$TeO_2$ TELLURITE GLASS SYSTEM

M. M. UMAIR, A.K.YAHYA*
Faculty of Applied Sciences, UniversitiTeknologi MARA, 40450 Shah Alam, Malaysia

Telluro-niobate$x$$Nb_2O_5$-(20-$x$)BaO-80$TeO_2$ glass system was prepared by melt-quenching method. Elastic, structure, and optical properties of the glass systems were measured using ultrasonic velocity measurement, Raman spectroscopy and UV-Vis spectroscopy, respectively. Results showed that the longitudinal velocity, v_L and shear velocity, v_s and independent moduli, C_L and μ steadily increased with Nb_2O_5. The related moduli such as bulk modulus, K_e and Young's modulus, Y and also Debye temperature, θ_D showed similar behavior to C_L and μ. The increase of elastic moduliis suggested to be due to the increase of bridging oxygen (BO) via TeO_4 tbp formation compared to non-brindging oxygen (NBO) which was confirmed by Raman spectroscopy and these results indicate the stabilizer effect of Nb_2O_5. Optical energy gap, E_{opt} was found to decrease with Nb_2O_5which is suggested to be due to smaller difference between HOMO and LUMO states of TeO_4 tbp compared to that of TeO_3 tp and the averaging effect of E_{opt} of constituent oxides. Meanwhile, Urbach energy, E_u decreased with Nb_2O_5 content indicating reduction in disorder of the glass structure.

(Received April 5, 2015; Accepted June 5, 2015)

Keywords: Tellurite glass;Elastic properties; Raman spectroscopy; Optical properties; Nb_2O_5

1. Introduction

Tellurite glasses have attracted much interest in the application of optical devices due to their high third-order nonlinear optical susceptibilities[1-4], high refractive index[5-8], high dielectric constant [9-11] and also good chemical durability[12]. These properties make the glass suitable material for optical applications such as laser materials and fiber optics. Also, tellurite glass shows low maximum phonon energy[13-16], low glass transition temperature[17,18], low crystallization ability [19]and is non-hygroscopic[20]. The unit structure for this glass, TeO_4 is unique where it consists of Te element positioned in trigonal bipyramids (tbp) with a lone pair in the equatorial position [21-23]. Another unit structure for this glass is TeO_3, which consists of Te element positioned in trigonal pyramids (tp) with two equatorial Te-O bond, one axial Te-O bonds and a lone pair. Uniquely, TeO_2 is a conditional network former as it cannot form glass on its own but needs a modifier such as alkali metal, alkaline earth metal, transition metal, or rare earth to form glass.

Addition of Nb_2O_5 in tellurite glass has been suggested to introduce some kind of stabilizer effect on glass network formation.For (80-x)TeO_2-20Nb_2O_5-xZnO glass system, Nb_2O_5 was reported to enter the glass network as NbO_6 octahedral by connecting two neighbouring TeO_4 tbp[24].Nb_2O_5also plays a dual role in glass network modification, as network former or network modifier, depending on its concentration[25, 26]. The increase of Nb_2O_5 for TeO_2-Nb_2O_5-ZnO-NdO[27]and TeO_2-ZnO-Nb_2O_5-Er_2O_3[25] glass systems were reported to increase BO whilefor TeO_2-ZnO-Nb_2O_5 glass system [28],BO decreased for Nb_2O_5< 10 mol % but increased for Nb_2O_5> 10 mol %. Particularly, for 76TeO_2-20Nb_2O_5-4BaO glass[24], besides Nb_2O_5, the presence of BaO

*Corresponding author:ahmad191@salam.uitm.edu.my

was suggested to contribute to the increase in third order non linear susceptibility, χ^3. BaO showed strong network modifier character as reported for TeO-TiO-BaO[21]and TeO-BaO[29, 30] glass systems. However, Nb_2O_5in the $76TeO_2$-$20Nb_2O_5$-4BaO glass system[24]was fixed and therefore, the structural change in the glass systemdue to the presence of Nb_2O_5/BaO is not very clear.Thus, further investigation on BaO-Nb_2O_5-TeO_2 glass system is essential to elucidate glass structure modification due to Nb_2O_5.

On the other hand, ultrasonic study in conjunction with Raman and/or FTIR spectroscopy is one of the best tools to investigate the influence of glass network modification on rigidity, stiffness as well as elastic properties of the glass [26,27,28, 31-41]. Glass network modification was reported to show very close correlation to elastic behavior of glass. Increase of TeO_4 tbp formation was suggested to enhance elastic properties due to formation of bridging oxygen as shown for xTiO$_2$-(50-x)V_2O_5-50TeO_2[38], xSm$_2$O$_3$-(35-x)V_2O_5-65TeO_2[37] and xWO$_3$-5ZrO-(95-x)TeO_2[7] tellurite glass systems. Meanwhile, the increase in TeO_3 tp formation which indicate increase in NBO of glass network weakens rigidity as shown by studies on xK$_2$O-(20-x)WO$_3$-60TeO_2[42], ,xNa$_2$O-(35-x)V_2O_5-65TeO_2[31] and xAg$_2$O-(50-x)V_2O_5-50TeO_2[43] glass systems. On the other hand, optical properties such as optical energy gap and refractive index can give good insight on structural and polarizability changes in glass[44-50]. It is known that Nb_2O_5 possess high polarizability due to the empty d shell [51] and is expected to give significant changes on optical properties. However, no elastic and optical studies on Nb_2O_5-BaO-TeO_2 glass system have been reported.

In this work, the effect of Nb_2O_5/BaO on elastic, structure and optical properties of $x$$Nb_2O_5$-(20-$x$)BaO-80$TeO_2$ glass system was investigated using ultrasonic velocity measurement, Raman and UV-Vis spectroscopy, respectively. All these three methods were analyzed and correlated to elucidate the changes in glass structure as a result of Nb_2O_5 addition.Also, further analysis on elastic properties using bulk compression and ring deformation models have been presented and discussed.

2. Experimental Detail

The $x$$Nb_2O_5$-20BaO-80$TeO_2$ glass samples with x= 0,5,10 and 15 mol % were prepared using the conventional solid state method and melt-quenching technique. Powders of Nb_2O_5, BaO and TeO_2 with purity >99.95%-99.99% was mixed and ground in an agate mortar in an hour to reach good homogeneity and fined grained mixture. The mixed batches were then melted for an hour at 900°C and quenched onto stainless steel plate before annealed at 400°C for 4 hours. The glasses were then ground into powder to meet the requirement of X-ray diffraction (XRD), Raman and UV-Vis measurements.

XRD analysis was performed using X'Pert Pro Panalytical diffractometer to confirm the amorphous nature of the glass samples. The density, ρ of the glass samples were determined by Archimedes principle with xylene as an immersion medium using the relation below:

$$\rho = \left(\frac{W_a}{W_a - W_b}\right)\rho_b \tag{1}$$

whereW_a is the glass sample weight in air, W_b is the glass sample weight in xylene and ρ_b is the density of xylene which is 0.861 g/cm^3. Raman spectra of the glass samples were recorded using HORIBA JOBIN HR800 LabRam spectrometer at room temperature with the wavelength range 100-1200 cm^{-1} and the excitation wavelength of 488nm (Ar^+ laser). Optical absorption spectra were recorded using Varian Cany 5000 UV-VIS-NIR spectrometer with wavelength range between 200-1000 nm at room temperature.

The samples were polished using fine sand paper to obtain parallel opposite faces to meet the requirement for ultrasonic velocity measurement. Ultrasonic velocity measurements were measured in both longitudinal and shear modes at room temperature by applying the pulse-echo overlap technique at 5MHz using Matec model 7700 system. The related elastic moduli were calculated using the equations:

Longitudinal modulus, $$C_L = v_L^2 \rho \quad (2)$$

Shear modulus, $$\mu = v_s^2 \rho \quad (3)$$

Bulk modulus, $$K_e = C_L - \left(\frac{4}{3}\right)\mu \quad (4)$$

Young's modulus $$Y = \frac{9K\mu}{3K + \mu} \quad (5)$$

Debye temperature, $$\theta_D = \left(\frac{h}{k_B}\right)\left(\frac{3PN_A}{4\pi V_a}\right)^{1/3} v_m \quad (6)$$

Hardness, $$H = \frac{(1-2\sigma)Y}{6(1+\sigma)} \quad (7)$$

Poisson's ratio, $$\sigma = \frac{C_L - 2\mu}{2(C_L - \mu)} \quad (8)$$

where h is the Planck's constant, k_B is the Boltzmann's constant, N_A is the Avogadro number, V_a is the molar atomic volume calculated from the effective molecular mass and the density (M/ρ), P is the number of atoms in the chemical formula and v_m is the mean sound velocity defined by the relation:

$$v_m = \left[\frac{3v_L^3 v_s^3}{v_L^3 + v_s^3}\right]^{1/3} \quad (9)$$

3. Results

XRD patterns for all the$x$Nb$_2$O$_5$-(20-x)BaO-80TeO$_2$; x=0, 5,10,15 mol % glass samples (Fig. 1) were observed to have no sharp peaks which confirm the amorphous nature of the samples. Values of density, ρ, molar volume, V_a, longitudinal velocity, v_L, shear velocity, v_s, longitudinal modulus, C_L and shear modulus, μ for all samples are tabulated in Table 1. The density, ρ shows steady decrease from 5.61 g cm^{-1} (x=0 mol %) to 5.25 g cm^{-1} (x=15 mol %) with Nb$_2$O$_5$ content (Fig. 2) while molar volume, V_a of the glasses showed steady increase from 28.22 cm^3 mol^{-1} (x=0 mol %) to 33.37 cm^3 mol^{-1} (x=15 mol %) (Fig. 2).

Table 1. Values of density, ρ, molar volume, V_a,longitudinal velocity, v_L, shear velocity, v_s, longitudinal modulus, C_L and shear modulus, μ of xNb_2O_5-(20-x)BaO-80TeO_2 glass samples.

x (%)	ρ (g cm^{-3}) ±0.03	V_a(cm^3/mol) ±0.02	v_L(km s^{-1}) ±0.01	v_s (km s^{-1}) ±0.01	C_L (GPa) ±0.4	μ (GPa) ±0.2
0	5.61	28.22	3.19	1.34	57.2	10.0
5	5.45	30.09	3.36	1.42	61.4	11.0
10	5.29	32.06	3.53	1.54	65.9	12.6
15	5.25	33.37	3.69	1.61	71.7	13.7

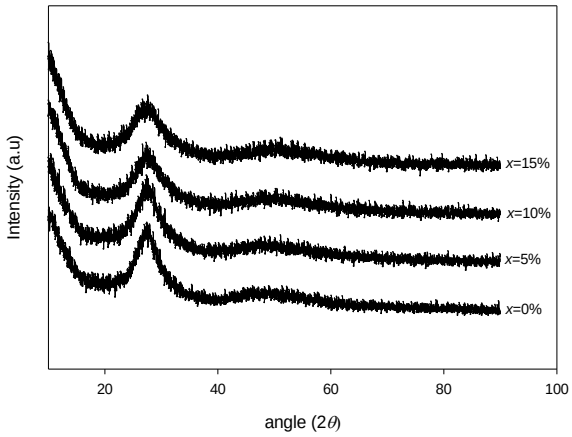

Fig. 1. XRD patterns of xNb_2O_5-(20-x)BaO-80TeO_2 glass samples.

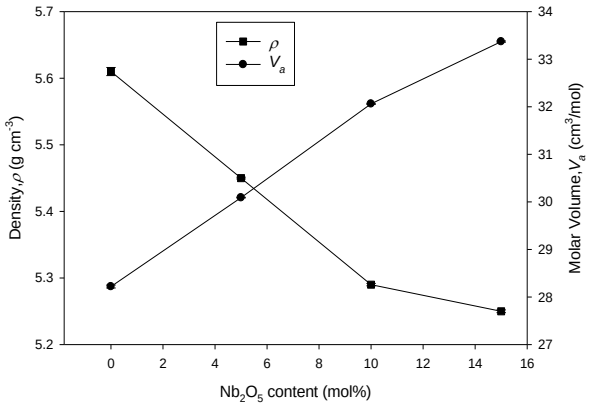

Fig. 2. Density (ρ) and molar volume (V_a) of xNb_2O_5-(20-x)BaO-80TeO_2 glass samples.

Fig. 3 shows Raman spectra of the $x$$Nb_2O_5$-(20-$x$)BaO-80$TeO_2$ glass samples for x=0,5,10,15 mol%. Four obvious peaks were observed in the spectra which is at 450-470 cm^{-1}, 660-663 cm^{-1}, 743-763 cm^{-1} and 879-883 cm^{-1}. As reported in previous structural studies on niobate tellurite glasses [25,27,28] the 450-470 cm^{-1} peak was assigned to asymmetric stretching and bending vibration of Te-O in TeO_4 trigonal bipyramid (tbp) and in the present work, this peak was observed to increase in intensity, broadening and shifted to lower frequency with addition of Nb_2O_5. Meanwhile, the peak of 660-663 cm^{-1} was assigned to symmetric vibration of Te-O in TeO_4tbp and this peak was also observed to increase in intensity with addition of Nb_2O_5 content. The 743-763 cm^{-1}peak which was assigned to TeO_3 trigonal pyramid showed decrease in intensity as Nb_2O_5 content increased. On the other hand, 879-883 cm^{-1}peak which refer to stretching vibration of Nb-O in NbO_6 octahedral [25,27,28,52] was observed in samples x=5-15 mol % only and this peak showed slight increase as $Nb_2O_5$was increased.

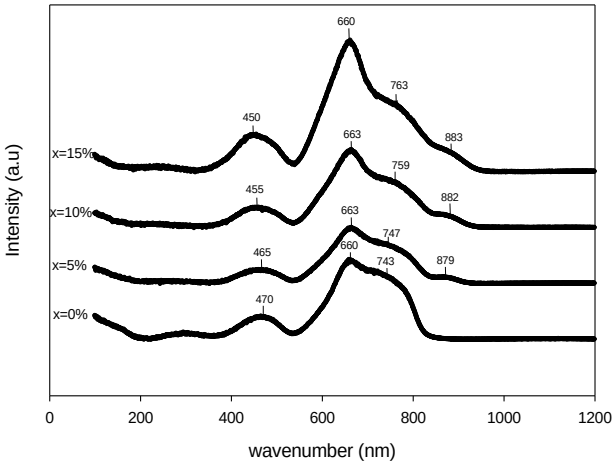

Fig. 3. Raman spectra of xNb_2O_5-(20-x)BaO-80TeO_2 glass samples.

Fig. 4 shows the behavior of longitudinal velocity, v_L and shear velocity, v_s as Nb_2O_5 content increased. The addition of Nb_2O_5 caused gradual increase in v_L from 3.19 km s^{-1}(x= 0 mol %) to 3.69 km s^{-1}(x=30 mol %) and also in v_s from 1.34 km s^{-1}(x=0 mol %) to 2.61 km s^{-1} (x=30 mol %). Meanwhile, longitudinal modulus, C_L and shear modulus, μ also show similar behavior with v_L and v_s (Fig. 5) with increases from 57.24 GPa (x=0 mol %) to 71.66 GPa (x=30 mol %) for C_L and form 10.04 GPa (x=0 mol %) to 13.67 GPa (x=30 mol %), for μ. Table 2 represent the values of bulk modulus, K_e, Young's modulus, Y, hardness, H, Poisson's ratio, σ, Debye temperature, θ_D and mean velocity, v_m. K_e steadily increased from 43.85 GPa to 53.43 GPa (Fig. 6) while Y also shows similar behavior with increase from 27.98 GPa to 37.79 (Fig. 6) as Nb_2O_5 content increased. On the other hand, hardness, H showed small increase with values between 0.71 GPa (x=0 mol %) and 4.99 GPa (x=15 mol %) (Fig. 7) while Poisson's ratio (σ) showed small decrease (Fig. 7) with the addition of Nb_2O_5. Fig. 8 showed the behavior of the Debye temperature, θ_D and mean velocity, v_m whereby both gradually increased with Nb_2O_5.

Table 2. Values of bulk modulus, K_e, Young's modulus, Y, hardness, H, Poisson's ratio, σ, Debye temperature, θ_D and mean velocity, v_m of xNb_2O_5-(20-x)BaO-80TeO_2 glass samples.

x (%)	K_e(GPa) ±1.0	Y(GPa) ±1.8	H(GPa) ±0.1	σ ±0.01	θ_D(°C) ±0.6	v_m(km s^{-1}) ±0.01
0	43.9	28.00	0.7	0.40	101.8	1.88
5	46.8	30.5	0.8	0.39	108.6	1.99
10	49.2	34.7	1.0	0.38	118.3	2.16
15	53.4	37.8	1.1	0.38	125.3	2.27

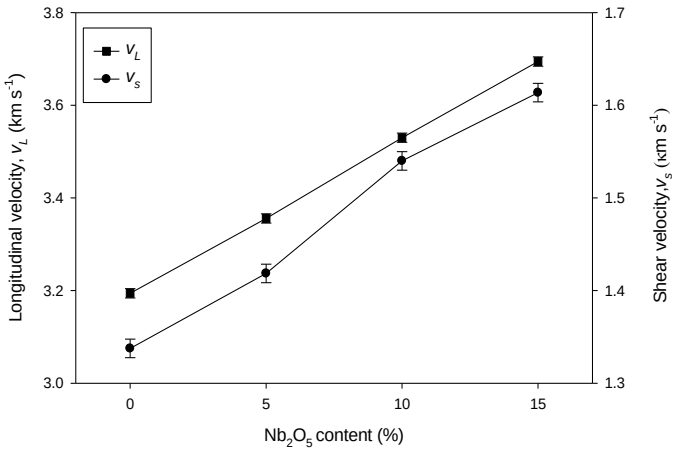

Fig.4. Longitudinal velocity, v_L and shear velocity, v_s of xNb_2O_5-(20-x)BaO-80TeO_2 glass samples.

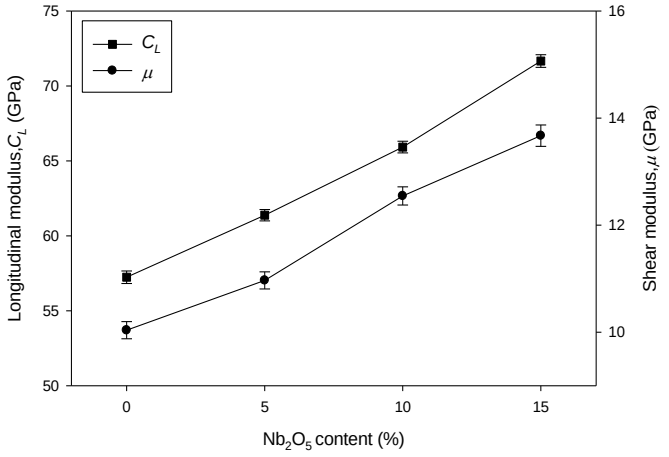

Fig.5. Longitudinal modulus, C_L and shear modulus,μ of xNb_2O_5-(20-x)BaO-80TeO_2 glass samples.

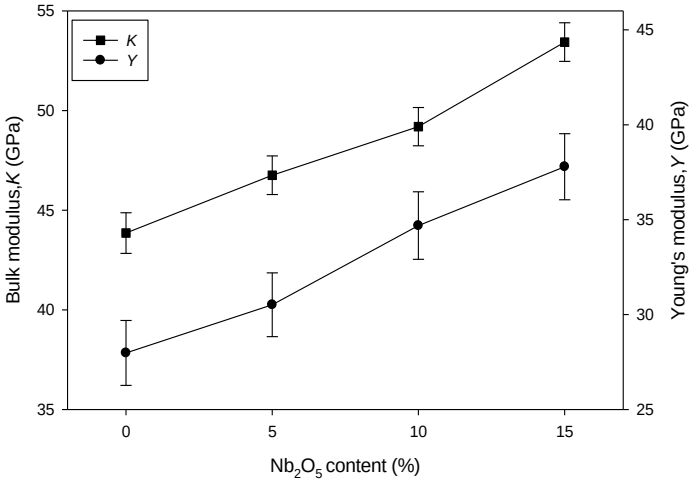

Fig.6. Bulk modulus, K_e and Young's modulus, Y of xNb_2O_5-(20-x)BaO-80TeO_2 glass samples.

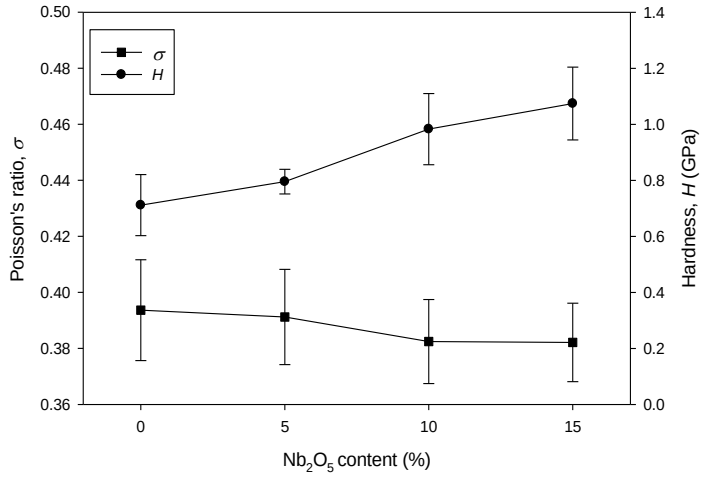

Fig.7. Hardness, H and Poisson's ratio, σ of xNb_2O_5-(20-x)BaO-80TeO_2 glass samples.

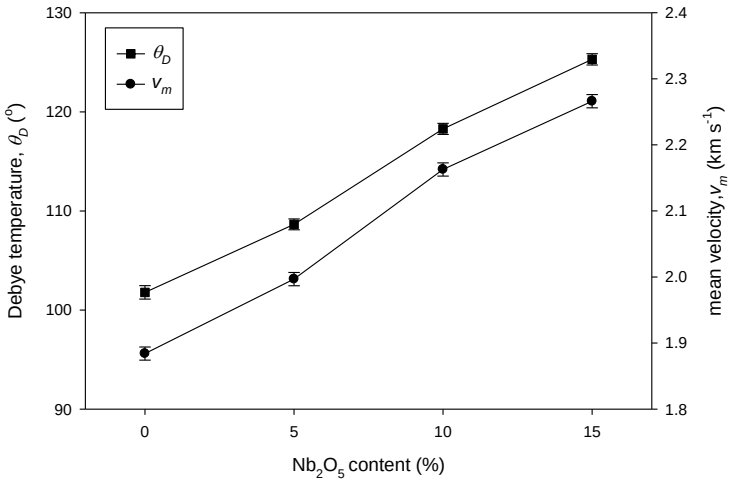

Fig.8. Debye temperature, θ_D and mean velocity, v_m of xNb_2O_5-(20-x)BaO-80TeO_2 glass samples.

A quantitative interpretation of the experimental elastic properties of the $x$$Nb_2O_5$-(20-$x$)BaO-80$TeO_2$ glass system can be further analyzed using the bulk compression model in conjunction with the ring deformation model. In the bulk compression model, it is assumed that the compression is isotropic in all directions with change in bond length without altering bond angle [23]. The theoretical bulk modulus, K_{bc}, was computed using the relation [53]:

$$K_{bc} = \frac{N_A}{9V_a} \sum \left(x n_f r^2 F \right)_n \tag{10}$$

where N_A is the Avogadro number, n_f is the cation coordination number, r is the bond length, F is the stretching force constant of oxide and$n$ is the mole fraction of component oxide. For this glass system, K_{bc} decreased with the addition of Nb_2O_5 content from 89.84 GPa (x=0 mol%) to 78.20 GPa (x=15 mol%). Fig.9 shows the behavior of K_{bc}/K_e with respect to the Nb_2O_5 content and shows the K_{bc}/K_e steadily decrease from 2.05 (x=0 mol %) to 1.46 (x=15 mol %). On the other hand, the ring size, l is calculated using relation[53]:

$$l = [\frac{K_e}{0.0106 F_a}]^{-\frac{1}{3.84}} \tag{11}$$

where K_e is the experimental bulk modulus and F_a is the average stretching force constant of glass which was calculated using equation [54]:

$$F_a = \frac{\sum (x n_i F)_n}{\sum (x n_i)_n} \tag{12}$$

The average ring size, l was observed to show a slight decrease(Fig. 9)between 0.467 nm (x=0 mol %) and 0.455 nm (x=15 mol %).The average ideal cross-link density, $\bar{n}_c$ was calculated using equation [53]:

$$\bar{n}_c = \frac{1}{\eta} \sum_i (n_c N_c) \tag{13}$$

wheren_c is the number of bridging bonds per cation minus two , N_c is the number of cations per glass formula unit and η is the total number of cations per glass formula unit. It was observed that the $\bar{n}_c$ steadily increased with addition Nb_2O_5 and the values lie between 2.40 (x=0 mol %) to 2.61 (x=15 mol %)(Table 4).

Table 3. Coordination number, n_f, bond length, r, first order stretching force constant, F and of the oxides of TeO_2, Nb_2O_5 and BaO.

Oxide	n_f	r (nm)	F (N m^{-1})
TeO_2 (Saddeek 2005)	4	0.199	216
Nb_2O_5 (Saddeek et al 2009)	6	0.170	346
BaO (Saddeek 2005)	6	0.194	232

Table 4. The values of theoretical bulk modulus, K_{bc}, ratio K_{bc} / K_e, average ring size, l and average cross-link density, $\bar{n}_c$ of xNb_2O_5-(20-x)BaO-80TeO_2 glass samples.

x (mol %)	K_{bc} (GPa) ±0.04	K_{bc}/K_e ±0.03	l (nm) ±0.01	$\bar{n}_c$
0	89.84	2.05	0.47	2.40
5	85.08	1.82	0.46	2.48
10	80.62	1.64	0.46	2.55
15	78.20	1.46	0.45	2.61

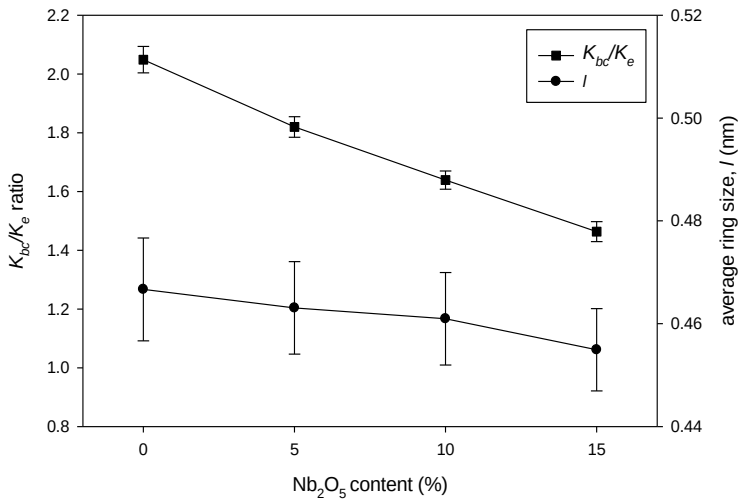

Fig.9 K_{bc}/K_e ratio and average atomic ring size, l of xNb_2O_5-(20-x)BaO-80TeO_2 glass samples.

Optical energy gap, E_{opt} of the $x$$Nb_2O_5$-(20-$x$)BaO-80$TeO_2$ glass samples were determined using equation [55]:

$$\alpha(\omega) = \frac{A(\hbar\omega - E_{opt})^p}{\hbar\omega} \tag{14}$$

where α is the absorption coefficient near the fundamental absorption edge of each spectrum, E_{opt} is the optical band gap in eV, A is a constant and p is an index which can be assumed to be 1/2, 3/2,2 or 3, depending on the nature of the electronic transition responsible for absorption. For amorphous materials, p=2 as absorption by indirect transition is most applicable according to Tauc relations [55]. The value of E_{opt} can be obtained from the above equation by extrapolating the α to zero absorption in the $(\alpha h\nu)^{1/2}$ vs $h\nu$ as shown plot in Fig. 10. The E_{opt} shows decrease from 2.93 eV (x=0 mol%) to 2.58 eV (x=15 mol%). (Fig. 11). On the other hand, in amorphous materials, band tailing exist in the forbidden energy band gap [51,55,56]. The band tailing which also known as Urbach energy can be determined using Urbach Rule [55]:

$$\alpha(\omega) = \alpha_o \exp[\frac{\hbar\omega}{E_u}] \tag{15}$$

where α_o is a constant and E_u is the width of the band tails of electron states in the forbidden band gap. The values of E_u were obtained from the reciprocal of the slope of the linear region of the curve (Urbach region) in the ln α vs $h\nu$ plot. The E_u was observed to increase at initial addition of 5 mol % of Nb_2O_5 from 0.70 eV (x=0 mol %) to 0.79 eV (x= 5 mol %) followed by large decrease to 0.55 eV (x>5 mol%). (**Fig. 11**).

Table 5. Values of optical band gap, E_{opt}, Urbach energy, E_u and refractive index, n of xNb_2O_5-(20-x)BaO-80TeO_2 glass samples.

x (%)	E_{opt} (eV)	E_u (eV)	n
0	2.93	0.70	2.42
5	2.75	0.79	2.47
10	2.67	0.55	2.49
15	2.58	0.58	2.52

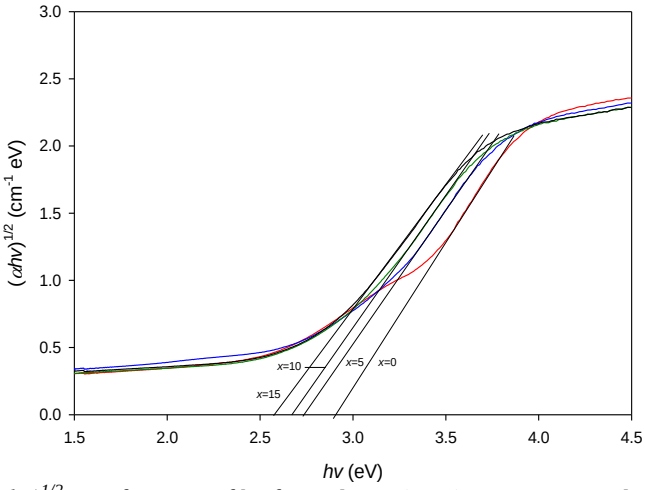

Fig.10. $(\alpha h\nu)^{1/2}$ as a function of hv for xNb_2O_5-(20-x)BaO-80TeO_2 glass samples.

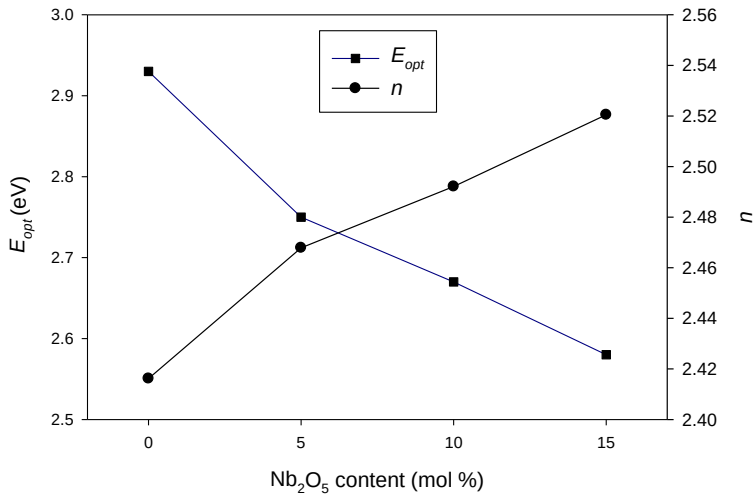

Fig.11. Optical band energy, E_{opt} and Urbach energy, E_u of xNb_2O_5-(20-x)BaO-80TeO_2 glass samples.

The values of refractive index, *n* were calculated by using the following relation [55]:

$$\left(\frac{n^2-1}{n^2+2}\right)=1-\sqrt{\frac{E_{opt}}{20}} \tag{16}$$

Our calculation showed *n* increased with addition of Nb_2O_5 content from 2.42 (*x*=0 mol %) to 2.52 (*x*=30 mol%) (Table 5).

4. Discussion

Analysis on density is important in glass studies to identify structural compactness [25,33]. In the present work, the change in ρ has been analyzed using the well-known formula, $\rho=M/V_a$ where *M* is the molecular mass while V_a is the molar volume of the glass samples. The decrease in ρ (Fig. 2) indicates decrease in compactness of the glass[25] and this is due to the increase in molar volume, V_a as a result of replacement of smaller BaO (26.80 cm^3/mol) by larger Nb_2O_5 (57.78 cm^3/mol).

The change in longitudinal velocity, v_L and shear velocity, v_s due to addition of Nb_2O_5 indicates that the elastic properties of this glass system are sensitive to the composition of the glass. The behavior of v_L and v_s were analyzed based on equation (2) and (3) where the ultrasound velocities are dependent on the independent moduli, C_L and μ and density, ρ. In the present work, the increase in ultrasound velocities was due to both increase in independent moduli and decrease in ρ. However, the larger percentage change of independent moduli (ΔC_L=25.20 % and $\Delta\mu$=36.21 %) in comparison wasρ which is 6.42 % gives insight of the dominant influence of both independent modulus on ultrasound velocities of the glass system.

On the other hand, the increase in intensity of asymmetric TeO_4 tbp (450-470 cm^{-1}) and symmetric TeO_4 tbp (660-663 cm^{-1} peak) (Fig. 3) obviously indicates increase in bridging oxygen (BO) [25,28]. Meanwhile, the intensity of TeO_3 tp peak showed decrease with addition of Nb_2O_5 and this indicates decrease in formation of non-bridging oxygen (NBO) [25]. On the other hand, the small increase in NbO_6 peak (879-883 cm^{-1}) indicates some increase in formation of NBO. Nevertheless, the obvious increase in intensity of TeO_4 tbp (450-470 cm^{-1} and 660-663 cm^{-1}peaks) indicates progressive formation of BO in comparison to NBO.

Elastic properties are considered important for the selection of glasses for a particular application as it gives valuable information on stiffness and rigidity [28,31,32,34,35,41]. The gradual increase in C_L and μ (Fig. 5) indicates the increase in stiffness and rigidity of the glass system, respectively [34,57]. The increase is suggested to be due to the increase in BO formation which is attributed to Nb_2O_5 addition concurrent with the decrease of network modifier, BaO. The formation of BO as a result of Nb_2O_5 addition was also reported for $x$$Er_2O_3$-15ZnO-(10-$x$)$Nb_2O_5-75TeO_2$[25], xPbO-(0.3-x)Nb_2O_5-0.7TeO_2[52] and $x$$Nd_2O_5$-15ZnO-(10-$x$)$Nb_2O_5-75TeO_2$[27] glass systems while formation of NBO as a result of BaO addition was reported for 80TeO_2-20ZnO-(x-20)BaO[58] and TeO_2-V_2O_5-BaO [59] glass systems.The increase in rigidity and stiffness together with BO formation indicates that Nb_2O_5 enters and stabilizes the glass network [24].Also, the increasing rigidity with Nb_2O_5 addition may be due to the reduction of stronger modifying BaO in comparison to Nb_2O_5 modifier.

Bulk modulus, K_e is a measure of material's resistance to uniform compression [23]. The steady increase in K_e reflects the increase in rigidity and stiffness of this glass. Meanwhile, Young's modulus, Y which is defined as the ratio of linear stress to linear strain showed gradual increase with Nb_2O_5 (Fig. 6) indicating increase in stiffness of the glass [34, 57]. In addition, the behavior of Y was observed to show similar behavior to C_L and μ and this gives insight on the influence of the independent moduli on Y. Poisson's ratio, σ is an essential parameter to study elastic properties of solid materials. It is defined as a ratio between lateral and longitudinal strains produced when a tensile force is applied [36]. Ideally, the decrease in $\sigma$is followed by an increase in actual cross link densityand vice versa as reported for $x$$TiO_2$-(50-$x$)$V_2O_5-50TeO_2$ [38], $x$$Fe_2O_3$-(20-$x$)ZnO-80$TeO_2$ [32] and $x$$Sm_2O_3$-(35-$x$)$V_2O_5-65TeO_2$ [37] glass systems. Therefore, the decrease in σ (Fig. 7) indicates increase in actual cross link in the glass system. This suggests that the increase in elastic moduli may also be contributed by the increase in cross link which consequently increase the stiffness and rigidity of the glass.

Debye temperature, θ_D represents the temperature where all modes of vibration are excited [36] and it is an important parameter for a solid. θ_D also reflects strength of bonds [60], rigidity [28,31,33] and stiffness [34,57] for the glass material. θ_D was analyzed based on equation (7) where it is depends on number of atoms in the chemical composition, P, molar volume, V_a or mean velocity, v_m. In the present work, the increase in θ_D(Fig. 8) may be due to the increase in P and v_m. However, θ_D was found to show similar behavior to v_m (Fig. 8) and thus this suggests that θ_D is strongly influenced by v_m. The dominant influence of v_m in θ_D indicates the increase in θ_D reflects the glass's rigidity. Such indication was also reported for xZnO-45PbO-(55-x)V_2O_5[34], $x$$WO_3$-20PbO-(80-$x$)$TeO_2$ [33] and $x$$Fe_2O_3$-(20-$x$)ZnO-80$TeO_2$ [32] glass systems.Previously, T. Hayakawa et al (2010) reported that the χ^3 increased as TeO_4 tbp increased in their studied glass system. The reportwas also supported by ab initio molecular orbital calculation result which showed higher polarizability of TeO_4 tbp compared to TeO_3 tp[26,61]. Thus our Raman analysis and elastic moduli results suggest some kind of correlation between rigidity and $\chi^3$for the glass system.

Analysis using the bulk compression model shows that the values of K_e were always smaller compared to K_{bc} indicating the energy required for the compression was less compared to ideal isotropic compression [23]. However, the decrease in K_{bc}/K_e ratio with addition of Nb_2O_5 (Fig. 9) indicates increase in ideal isotropic compression at the expense of ring deformation[42,60]. As described by Afifi and Gaafar (2004), the value of K_{bc}/K_e=1 indicates compression occur via ideal compression while K_{bc}/K_e = 3-10 indicates bond bending process is involved during compression. In this present work, K_{bc}/K_e value is close to 2 which indicate the main compression mechanism remains ideal compression. In addition, the behavior of K_{bc}/K_e follow suit with average ring size, l (Fig. 9) indicating decrease in ring deformation with Nb_2O_5 addition. Similar observations were reported for xK$_2$O-(20-x)WO$_3$-80TeO$_2$ (Sidkey and Gaafar 2004), xNa$_2$O-(35-x)V$_2$O$_5$-65TeO$_2$ [31] and xSm$_2$O$_3$-(35-x)V$_2$O$_5$-65TeO$_2$ [37].

Generally, a decrease in E_{opt} can be due to increase in NBO where electrons were held less tight compared to BO[51,55]. Intriguingly, in the present study, the decrease in E_{opt} was accompanied by the increase of BO. Nevertheless, the decrease in E_{opt} due to increase in TeO_4 have been suggested for xFe$_2$O$_3$-(100-x)[4TeO$_2$-PbO$_2$[62], 68TeO$_2$-5Nb$_2$O$_5$-20ZnO-7PbO[63], 70TeO-10Nb$_2$O$_5$-20PbO [52] and 50(6TeO$_2$-4V$_2$O$_5$)-50PbO [17] glass systems where ab-initio molecular orbital calculation shows that the difference between highest occupied molecular orbital (HOMO) and lowest unoccupied molecular orbital (LUMO) state of TeO_4 tbp is small compared to that of TeO_3 tp. Therefore, the decrease in E_{opt} in the present glass system is suggested to be due to the increase in TeO_4 tbp. Also, G. Upenderet. al. (2010) suggested that the decrease in E_{opt} may not be related to structural change but contributed by the E_{opt} of constituent oxides. If constituent oxides is considered to affect E_{opt} of the presently studied glass system, the replacement of Nb_2O_5(E_{opt}=3.30 eV)[52] with BaO (E_{opt}=3.45 eV)[64] contributes to the decrease in $E_{opt.}$of the glass system.On the other hand, amorphous materials possess band tail energy due to their disordered structure [51,55,56]. This band tail, also known as the Urbach energy, E_u is determined using the Urbach rule and its increase indicates increase in degree of disorder of the amorphous structure [51,55,56]. In the present work, the decrease in E_u (Table 5) indicates reduction of defects in this glass system as Nb_2O_5 increased. Generally, refractive index of tellurite glass shows increase with increase in NBO formation. However in the present study, n showed increase with increase in BO formation as discussed earlier in our Raman analysis. Interestingly, several reports for TlO-TeO$_2$[66]and 68TeO$_2$-5Nb$_2$O$_5$-20ZnO-7PbO [64] glass systems suggest that the increase in n was due to increase in TeO_4 tbp which possesses about 20% higher mean polarizability compared to that of TeO_3 tp as computed by ab initio molecular orbital calculation. Thus the increase in n for xNb$_2$O$_5$-(20-x)BaO-60TeO$_2$ glass system may be to be due to the increase in TeO_4 tbp which has higher mean polarizability in comparison to TeO_3 tp.

5. Conclusion

Elastic, structural and optical properties of the xNb$_2$O$_5$-(20-x)BaO-60TeO$_2$ glass system have been investigated. Addition of Nb_2O_5 at the expense of BaO caused increase in ultrasound velocities and elastic properties indicating increase in rigidity and stiffness of the glass system. Raman analysis showed predominant formation of BO via TeO_4tbp group. The results suggest Nb_2O_5 enters and stabilizes the glass network. On the other hand, K_{bc}/K_e ratio decreased with Nb_2O_5 indicating reduction of ring deformation upon compression due to reduction in average ring size. The decrease in optical band gap, E_{opt} is suggested to be due to the smaller difference between HUMO and LUMO states of TeO_4 tbp compared to that of TeO_3 tp and to the averaging effect of E_{opt} of constituent oxides. Addition of Nb_2O_5 also caused refractive index to increase and Urbach energy to decrease.

Acknowledgement

A.K. Yahya would like to acknowledge research grant from Ministry of Education (MOE), grant no. 600-RMI/RACE 16/6/2(1/2013).

References

[1] T. Xu, F. Chen,S. Dai, X. Shen, X. Wang, Q. Nie, C. Liu, K. Xu, J. Heo. J. Non-Cryst. Solids, **357**, 2219 (2011).
[2] F. Chen, T. Xu, S. Dai, Q. Nie, X. Shen, J. Zhang, X. Wang, Optical Materials **32**, 868(2010).
[3]E. Yousef, M. Hotzel, C. Russel. J. Non-Cryst. Solids, **353**, 333 (2007).
[4]N. Ghribi, M. Dutreilh-Colas, J.R. Duclère, T. Hayakawa, J. Carreaud, R. Karray, A. Kabadou, P. Thomas.J. Alloy. Compd. **622**, 333 (2015).
[5]E. S. Yousef and B. Al-Qaisi.Solid State Sciences,**19**, 6 (2013).
[6]R. El-Mallawany, M. Dirar-Abdalla, I. A. Ahmed.Mater.Chem. Phys. **109**, 291 (2008).
[7]El Sayed Yousef, Amin El-Adawy, N. El Koshkhany, E. R. Shaaban. J. Phys. and Chem. Solids,**67**,1649(2006).
[8]N, Elkhoshkhany, RafikAbbas, R. El-Mallawany,A. J. Fraih. Ceramics International, **40**, 14477(2014).
[9]Mohamad M. Ahmad., El Sayed Yousef,El Sayed Moustafa.Physica B, **371**, 74(2006)
[10]D. Dutta, M. P. F. Graca, M. A. Valente, S. K. Mendiratta. Solid State Ionics. **230**,66(2013)
[11]M. Prashant Kumar, T. Sankarappa, B. Vijaya Kumar,N. Nagaraja.Solid State Sciences, **11**, 214 (2009)
[12]A. Belwalkar, H. Xiao, W. Z. Misiolek, J. Toulouse. J. Mater. Process.Technol. **210**, 2016 (2010).
[13]Vineet Kumar Rai, KaushalKumar, S B Rai.Optical Materials.**29**, 873 (2007).
[14]ShiqingXu, HongtaoSun, ShixunDai, JunjieZhang,ZhonghongJiang. Solid State Communications,**133**, 89 (2005).
[15]XunsiWang, LirenLiu, QiuhuaNie, TiefengXu, Xiang Shen, ShixunDai and Xianghua Zhang SpectrochimicaActa Part A,**67**, 1025 (2007).
[16]C. Zhao, G.F. Yang, Q.Y. Zhang,Z.H.J. Jiang. J. Alloy. Compd, **461**, 617 (2008)
[17]S. Rada, M. Neumann,E.Culea.Solid State Ionics, **181**, 1164 (2010)
[18]A. Abd. El-Moneim. Mater. Chem. Phys. **73**, 318 (2002)
[19]N.V. Ovcharenko,T. V. Smirnova.J. Non-Cryst. Solids.**291**, 121 (2001)
[20]R. El-Mallawany. Mater. Chem. Phys. **53**, 93 (1998)
[21]J.C. Sabadel,P. Armand,D. Cachau-Herreillat,P. Baldeck, O. Doclot, A. Ibanez, E. Philippot. J. Solid State Chem.,**132**, 411 (1997)
[22]U. Hoppe, E. Yousef, C. Russel, J. Neuefeind,A.C. Hannon. Solid State Communications, **123**, 273 (2002).
[23]R. El-Mallawany, Tellurite Glasses Handbook, Physical Properties and Data, CRC Press LLC, FL, USA, (2002)
[24]TomokatsuHayakawa, Masahiko Hayakawa, Masayuki Nogami,Philippe Thomas. Optical Materials,**32**, 448 (2010)
[25]N. Baizura,A.K. Yahya.J Non-Cryst.Solids.,**357**, 2810 (2011)
[26]U. Hoppe, E. Yousef,C. Russel, J. Neuefeind, A.C. Hannon. J. Phys Condens. Matter, **16**, 1645 (2004)
[27]V. Kamalaker, G. Upender, Ch. Ramesh and V. Chandra.SpectrochimicaActa Part A, **89**, 149 (2002)
[28]N.B. Mohamed, A.K. Yahya, M.S.M. Deni, S.N. Mohamed, M.K. Halimahand H.A.A. Sidek. J. Non-Cryst Solids,**356**, 1626 (2010)
[29]Takao Sekiya, Norio Mochida,Atsushi Ohtsuka.J. Non-Cryst. Solids,**168**, 106 (1994)
[30]A. NisharaBegum,V.Rajendran.Mater.Lett.,**61**,2143 (2007).
[31] M.M. Umair,A.K. Yahya.Mater.Chem. Phys.,**142**,549 (2013).
[32] S. Azianty, A.K. Yahya, M.K. Halimah. J. Non-Cryst. Solids,**358**,1562 (2012).
[33] S.Azianty, A.K. Yahya. J. Non-Cryst. Solids,**378**,234 (2013).
[34]S.Laila, S.N.Supardan,A.K. Yahya. J Non-Crystal. Solids**367,** 14(2013).
[35] S. Laila, A.K. Suraya, A.K. Yahya. ChalcogenideLatters, **11**,91 (2014).
[36]M.A.Sidkey, R.E1-Mallawany, R.I Nakhla,A. AbdE1-Moneim. J. Non-Cryst. Solids **215**,75(1997).

[37] M.A Sidkey, A .AbdEl-Moneim, L. AbdEl-Latif.Mater. Chem. Phys. **61**,103 (1999)
[38] R. El-Mallawany, N. El-Khoshkhany,H. Afifi.Mater.Chem. Phys.,**95**, 321 (2006).
[39] Yasser B. Saddeek.Mater.Chem. Phys.,**91**, 146 (2005).
[40] DariushSouri.Measurement,**44**, 1904 (2011).
[41] I.Z. Sapian, M.I.M. Yusof, A.K. Yahya.Chalcogenide Letters, **11**, 491 (2014).
[42] M.A. Sidkey, M.S.Gaafar.Physica B,**348**, 46 (2004).
[43] R. El-Mallawany, A. Abousehly, E. Yousef.J. Mater. Science Lett.,**19**,409 (2000).
[44]G. Upender, Ch. Sameera Devi, V.Chandra Mouli. Mater. Res. Bull.,**47**, 3764 (2012).
[45]G. Vijaya Prakash, D. Narayana Rao and A.K. Bhatnagar. Solid State Communications. **119**, 39 (2001).
[46]J.C.S. Moraes, J.A. Nardi, S.M. Sidel, B.G. Mantovani, K. Yukimitu, V.C.S. Reynoso, L.F. Malmonge, N. Ghofraniha, G. Ruocco, L.H.C. Andrade, S.M. Lima. J. Non-Cryst. Solids,**356**, 2146 (2010).
[47]A.H. Khafagy, A.A. El-Adawy, A.A. Higazy, S. El-Rabaie,A.S. Eid. J. Non-Cryst. Solids, **354**, 3152 (2008).
[48]Zahra Ashur Said Mahraz, M. R. Sahar and S.K. Ghoshal. J. Molecular Structure, **1072**, 238 (2014).
[49]R. S. Kundu, Sunil Dhankhar, R. Punia, Kirti Nanda, N. Kishore. J. Alloy. Compd. **587**, 66, (2014).
[50]H. Desirena, A. Schülzgen, S. Sabet, G. Ramos-Ortiz, E. de la Rosa, N. Peyghambarian. Optical Mater.,**31**, 784 (2009).
[51]Yanling Wang, Shixun Dai, Feifei Chen, Tiefeng Xu, Qiuhua Nie, Mater. Chem. Phys., **113**, 407 (2009).
[52]Jitka Ozdanova, Helena Ticha, Ladislav Tichy.Optical Mater., **32**, 950 (2010).
[53]B. Bridge, N.D. Patel, D.N. Waters.Phys. State Solids,**177**, 655 (1983).
[54]A.A. Higazy, B. Bridge.Phys. Chem. Glasses,**17**, 1 (1986).
[55]G. Upender, S. Ramesh,M. Prasad,V.G. Sathe, V.C. Mouli.J. Alloy. Compd., **504**, 468 (2010).
[56]TomoharuHasegawa. J. Non-Cryst. Solids,**357**, 2857 (2011).
[57]M.M. Umair, A.K. Yahya, M.K. Halimah, H.A.A. Sidek. J. Mater. Sci. Technol. **31**, 83 (2015).
[58]N Manikandan, AleksandrRyasnyanskiy,Jean Toulouse.J. Non-Cryst. Solids, **358**, 947 (2012).
[59]SungpingSzu,Fu-ShyangChang. Solid State Ionics,**176**, 2695 (2005).
[60]H. Afifi, S. Marzouk. Mater. Chem. Phys.,**80**,517 (2003).
[61]Jian Lin, Wenhai Huang, Zhengrong Sun, Chandra S. Ray,Delbert E. Day. J. Non-Cryst. Solids,**336,** 189 (2004).
[62]Simona Rada, Adriana Dehelean,Eugen Culea. J. Mol Model.,**17**, 2103 (2011).
[63]El Sayed Yousef, A.E. Al-Salami,Mario Hotzel. Bull. Mater. Sci.,**35**,961(2012).
[64]F.I.Ezema, P.E Ugwuoke. Pacific J. Sci. Technol.,**5**, 33(2004).
[65]B.Jeansannetas, S.Blanchandin, P.Thomas, P. Marchet, J.C. Champarnaud-Mesjard, T.Merle-MeHjean, B. Frit. J. Solid State Chem. **146**,329 (1999).